Structural and Dynamic Characterization of the Phosphotyrosine Binding Region of a Src Homology 2 Domain−Phosphopeptide Complex by NMR Relaxation, Proton Exchange, and Chemical Shift Approaches†

Steven M. Pascal,‡,§ Toshio Yamazaki,§ Alex U. Singer,‡,⊥ Lewis E. Kay,*,§ and Julie D. Forman-Kay*,‡

Biochemistry Research Division, Hospital for Sick Children, 555 University Avenue, Toronto, Ontario, M5G 1X8 Canada, Protein Engineering Network Centers of Excellence and Departments of Medical Genetics, Biochemistry and Chemistry, University of Toronto, Toronto, Ontario, M5S 1A8 Canada, and Division of Molecular and Developmental Biology, Samuel Lunenfeld Research Institute, Mount Sinai Hospital, 600 University Avenue, Toronto, Ontario, M5G 1X5 Canada

Received May 5, 1995; Revised Manuscript Received June 16, 1995⊗

ABSTRACT: Arginine side chains are often involved in protein−protein and protein−nucleic acid interactions. Due to a number of factors, resonance assignment and detection of NOEs involving the arginine side chains via standard NMR techniques can be difficult. We present here an approach to characterization of the interaction between a phosphopeptide (pY1021) and four arginine residues that line the phosphotyrosine-binding pocket of the C-terminal SH2 domain of phospholipase C-γ1 (PLCC SH2). Previously published [Pascal, S. M., et al. (1994) *Cell 77*, 461] NOE data provide a partial description of this interaction, including contacts between the aliphatic region of Arg 59 and the phosphotyrosine (pTyr) aromatic ring. Further characterization has now been accomplished by using ^{15}N and ^{13}C NMR relaxation studies of arginine N^{ϵ} and C^{ζ} spins, respectively, and proton exchange rates of arginine H^{ϵ} nuclei. Differences between the chemical shifts of the arginine guanidino groups of the free SH2 domain in imidazole and phosphate buffers or in complex with pY1021 have provided insight into specific interactions with the phosphate and the aromatic ring of the pTyr. The resulting data are consistent with the most stable hydrogen bonds to phosphate donated by the Arg 39 ϵ-NH and the two Arg 37 η-NH_2 groups and with pTyr aromatic ring interactions involving the Arg 39 and possibly the Arg 18 guanidino groups.

Src homology 2 (SH2)[1] domains are modular regions of approximately 100 residues that are present in many of the proteins involved in cell signaling [for reviews, see Koch et al. (1991), Cantley et al. (1991), and Pawson and Gish (1992)]. The function of these domains is to mediate protein−protein interactions by binding to phosphorylated tyrosine (pTyr) sites. Phospholipase C-γ1 (PLC-γ1) contains two SH2 domains (Rhee, 1991). The specific binding of the C-terminal SH2 domain (PLCC SH2) to the pTyr-1021 site of the platelet-derived growth factor receptor (PDGFR) activates the PLC-γ1 lipase function. The activated form of the molecule subsequently cleaves the membrane lipid phosphatidylinositol 4,5-bisphosphate (PIP_2) into inositol 1,4,5-triphosphate and 1,2-diacylglycerol, resulting in the activation of a cascade of signaling events.

The PLCC SH2 domain contains a large central β−sheet and an associated smaller β−sheet flanked by two α−helices (Pascal et al., 1994). Isolated PLCC SH2 binds tightly (K_D ~ 100 nM; Piccione et al., 1993; S. E. Shoelson, personal communication) to a 12-residue peptide (pY1021) of sequence DNDpYIIPLPDK, derived from the pTyr-1021 site of the PDGFR. The intermolecular interface of the PLCC SH2−pY1021 complex can be divided into two distinct regions: a phosphotyrosine-binding pocket and a hydrophobic groove that binds the six peptide residues C-terminal to the pTyr. The structure of the latter interface region has been well determined [0.5 ± 0.1 Å root mean square deviation (rmsd) of non-hydrogen atoms of an ensemble of calculated structures from the average structure; Pascal et al., manuscript in preparation] by solution NMR techniques, primarily based on interproton distance restraints derived from nuclear Overhauser effect (NOE) spectroscopy. In contrast, the phosphotyrosine-binding region, which primarily consists of four arginine side chain groups, has proven more difficult to characterize by standard NOE-based procedures (1.2 Å rmsd for all non-hydrogen atoms; Pascal et al., manuscript in preparation) due to a number of factors. First, the absence of protons attached to the phosphate group of the ligand implies that distance constraints in this region will be difficult to obtain from $^1H-^1H$ NOE experiments. Second, many of the arginine H^{η} and N^{η} chemical shifts are nearly degenerate, creating difficulties in the assignment of NOEs involving H^{η} protons. In addition, dynamic processes on the millisecond to microsecond time scale result in

† S.M.P. and T.Y. are the recipients of a Medical Research Council of Canada (MRC) Fellowship and a Human Frontiers Science Program Fellowship, respectively. This work was supported by grants from the National Cancer Institute of Canada (NCIC) to J.D.F.-K. and L.E.K., with funds from the National Cancer Society.

‡ Hospital for Sick Children

§ University of Toronto.

⊥ Mount Sinai Hospital.

⊗ Abstract published in *Advance ACS Abstracts,* August 15, 1995.

[1] Abbreviations: CPMG, Carr−Purcell−Meiboom-Gill: HSQC, heteronuclear single-quantum coherence; k_{ex}, exchange rate between conformers (in second^{-1}); NMR, nuclear magnetic resonance; NOE, nuclear Overhauser effect; PDGFR, platelet-derived growth factor receptor; PLC-γ1, phospholipase C-γ1; PLCC SH2, C-terminal phospholipase C-γ1 SH2 domain; ppm, parts per million; pTyr, phosphotyrosine; pY1021, the peptide DNDpYIIPLPDK derived from the pTyr-1021 site of the PDGFR; *S*, order parameter; SA, surface accessibility; SH2, Src homology 2; T_1, spin−lattice relaxation time; T_2, spin−spin relaxation time; $T_{1\rho}$, relaxation time of spin-locked magnetization; TPPI, time proportional phase incrementation; ω_{ex}, difference in chemical shift between two exchanging conformers (in radians second^{-1}).

0006-2960/95/0434-11353$09.00/0

significant intermediate exchange broadening and, thus, reduced intensity of many arginine aliphatic resonances. Rotation about the $N^{\epsilon}-C^{\zeta}$ bond can also cause broadening of the N^{η} and H^{η} resonances. The intensities of NOEs involving these broadened protons therefore are significantly reduced.

In order to further characterize interactions between the pY1021 ligand and the PLCC SH2 domain at the pTyr-binding site, arginine $^{15}N^{\epsilon}$ T_1 and T_2 relaxation times, steady state $^{15}N^{\epsilon}\{^1H^{\epsilon}\}$ NOEs, and $^{13}C^{\zeta}$ $T_{1\varrho}$ relaxation times have been measured. Interactions between the guanidino protons and nitrogens and the phosphotyrosine of the peptide have been investigated by observing $^{15}N^{\epsilon}$ and $^1H^{\epsilon}$ chemical shift changes in various buffer systems and measuring $^1H^{\epsilon}$ exchange rates with water. Where resolution permits, the chemical shift behavior of the η resonances has been analyzed as well. This approach may be valuable for the study of other intermolecular interactions in which arginine–ligand contacts play a key role, such as in other SH2 domain–phosphopeptide complexes and protein–DNA/RNA complexes (Pavletich & Pabo, 1993; Omichinski et al., 1993).

MATERIALS AND METHODS

NMR Spectroscopy. Expression, purification, and sample preparation of the PLCC SH2–pY1021 complex have been described previously (Pascal et al., 1994). NMR experiments were recorded on a 0.8 mM $^{15}N/^{13}C$-labeled PLCC SH2 sample with equimolar unlabeled pY1021 peptide at pH 5.7 in 100 mM sodium phosphate dissolved in 90% H_2O/10% D_2O at 30 °C, with carrier positions set to 100 (^{15}N), 4.73 (^1H), and 43 ppm (^{13}C) unless otherwise noted. Note that the phosphate group of pY1021 is almost completely in the −2 charge state in all samples since the pK_a of the less acidic proton is below 4.5 (A. U. Singer and J. D. Forman-Kay, manuscript in preparation). NMR spectra were acquired on a Varian UNITY 500 MHz spectrometer equipped with a triple-resonance, pulsed field gradient probe with an actively shielded z-gradient and a gradient amplifier unit, with the exception of the $^{15}N-^1H$ correlation spectra used to measure slow H^{ϵ} exchange with solvent D_2O and one set of T_2 relaxation experiments, which were recorded on a Varian UNITY+ 600 MHz spectrometer similarly equipped. Complex data were acquired in the indirect dimensions by the States–TPPI method (Marion et al., 1989a). All experiments incorporate pulsed field gradients to suppress artifacts and to assist in the elimination of the water resonance (Bax & Pochapsky, 1992; Kay, 1993). Gradient selection/enhancement (Kay et al., 1992; Muhandiram & Kay, 1994; Schleucher et al., 1993) was employed when appropriate. NMR spectra were processed using either commercially available software and in-house routines or the NMRPipe software system (Delaglio, 1993) and analyzed with the programs PIPP and CAPP (Garrett et al., 1991) on SUN Sparc stations. Many of the 2D data sets were linearly predicted in t_1, weighted by a 54° phase-shifted sine bell in t_1 and a 54° phase-shifted squared sine bell in acquisition, and zero filled twice in each dimension. Deconvolution of time domain data (Marion et al., 1989b) was used to eliminate residual solvent signal in some spectra.

Assignment. Assignments of arginine N^{ϵ}, H^{ϵ}, N^{η}, and H^{η} resonances of the PLCC SH2–pY1021 complex in phosphate buffer were obtained via Arg-$H^{\epsilon}(N^{\epsilon}C^{\delta})H^{\delta}$, Arg-$H^{\epsilon}(N^{\epsilon}C^{\zeta})$-$N^{\eta}$, and Arg-$H^{\eta}(N^{\eta}C^{\zeta}N^{\epsilon})H^{\epsilon}$ spectra acquired as described previously (Yamazaki et al., 1995). These experiments use exclusively through-bond connectivities to correlate $H^{\epsilon}-H^{\delta}$, $H^{\epsilon}-N^{\eta}$ and $H^{\eta}-H^{\epsilon}$ chemical shifts, respectively. Sequence specific assignment of arginine H^{δ} protons was achieved via a 3D H(CCO)NH TOCSY (Grzesiek et al., 1993; Logan et al., 1993; Montelione et al., 1992) with acquisition times of 25.6 ms and 64 complex points in t_1 (^1H), 19.4 ms and 32 complex points in t_2 (^{15}N carrier at 119 ppm), and 64.0 ms and 256 complex points in t_3 (^1H). A 13.3 ms ^{13}C DIPSI-2 mixing scheme (Shaka et al., 1988) using an 8.14 kHz field was employed. Mirror image linear prediction (Zhu & Bax, 1990) was used to extend the time domain in t_2. The H(CCO)NH TOCSY data were weighted by a 63° phase-shifted sine bell in t_1, a 90° shifted sine bell in t_2, and a 63° phase-shifted squared sine bell in acquisition and zero filled in each dimension. This spectrum was also used to monitor the relative relaxation properties of the aliphatic regions of the arginine side chains.

Assignments in Other Environments. Assignment of the guanidino resonances of a 0.3 mM ^{15}N-labeled PLCC SH2 sample with equimolar unlabeled pY1021 in 100 mM imidazole buffer at pH 6.0 was made by comparison of an $^{15}N-^1H$ correlation spectrum [Figure 1c, obtained with acquisition times of 26.7 ms and 128 complex points in t_1 (^{15}N) and 63.3 ms and 608 complex points in t_2 (^1H)] with the nearly identical $^{15}N-^1H$ correlation spectrum of the PLCC SH2–pY1021 complex in phosphate buffer, which has previously been assigned [compare Figure 1 of Yamazaki et al. (1995)].

Assignments for several H^{ϵ} and N^{ϵ} resonances of the free 0.3 mM PLCC SH2 domain in 100 mM imidazole (Figure 1a) and 100 mM phosphate (Figure 1b) buffered solutions at pH 6.0 were determined via titration of pY1021 peptide into the uncomplexed samples. At several steps during titration of the peptide, $^{15}N-^1H$ correlation spectra with acquisition times of 32.0 ms and 128 complex points in t_1 (^{15}N) and 64.0 ms and 512 complex points in t_2 (^1H) were obtained and used to monitor changes in H^{ϵ} and N^{ϵ} chemical shifts. Spectra of samples in imidazole buffer were acquired with gradient selection/enhancement in order to suppress t_1 noise arising from imidazole protons, while spectra of samples in phosphate buffer were acquired without sensitivity enhancement in order to maximize intensity from $N^{\eta}-H^{\eta}$ peaks. Chemical shifts of arginines 27, 30, 50, 91, and 96 were virtually unchanged during the course of the titrations. Thus, resonances of the free PLCC SH2 domain for these residues could be assigned immediately.

The Arg 37 H^{ϵ}, N^{ϵ}, H^{η}, and N^{η} resonances of free PLCC SH2 in phosphate buffer were also determined via the preceding titration. However, most of the cross-peaks from other residues in the pTyr-binding site (arginines 18, 39, and 59) could not be assigned in this manner since intermediate to slow exchange rates between peptide-bound and peptide-free conformations resulted in the disappearance or doubling of cross-peaks at partial titration points, with no obvious correlation between peaks. Instead, an H(CCO)NH TOCSY spectrum acquired with parameters similar to those for the H(CCO)NH TOCSY of the complex (see above) was used to determine the H^{δ} chemical shifts of these arginines in a 1.2 mM $^{15}N/^{13}C$-labeled free PLCC SH2 sample in 100 mM sodium phosphate at pH 5.8. The H^{δ} shifts were subsequently correlated with the H^{ϵ} shifts via an Arg-$H^{\epsilon}(N^{\epsilon}C^{\delta})$-

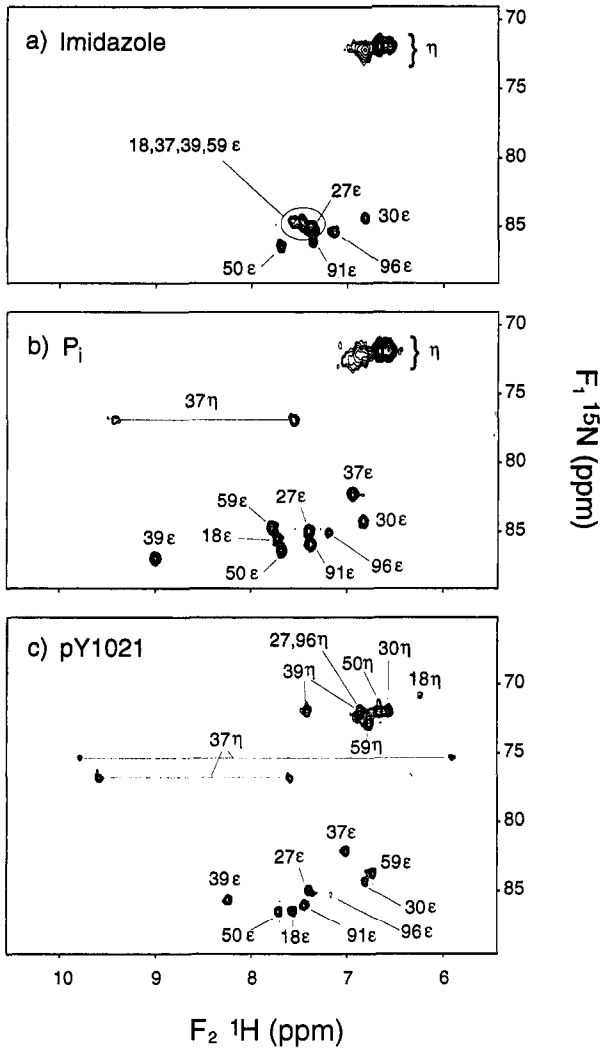

FIGURE 1: ^{15}N−^{1}H HSQC spectra of 0.3 mM PLCC SH2 (pH 6.0) in (a) 100 mM imidazole buffer, (b) 100 mM phosphate buffer, and (c) 100 mM imidazole buffer with 0.3 mM pY1021 peptide. N^ϵ−H^ϵ cross-peaks from arginines 18, 37, 39, and 59 lie within the oval in (a) and could not be assigned individually. Differences between chemical shifts from (a) and (b) indicate the effects of phosphate. Differences between (b) and (c) indicate the effects of the remainder of the phosphopeptide, excluding the phosphate.

H^δ experiment recorded with acquisition times of 16.0 ms and 64 complex points in t_1 (^{1}H) and 64.0 ms and 512 complex points in t_2 (^{1}H). In cases of overlapping H^δ shifts, a 100 ms mixing time, $^{15}N^\epsilon$-selective 2D ^{1}H−^{1}H NOESY spectrum with acquisition times of 21.3 ms and 128 complex points in t_1 (^{1}H) and 64.0 ms and 512 complex points in t_2 (^{1}H) was used to detect arginine H^ϵ−H^γ and H^ϵ−H^β NOEs. This experiment is similar to a 2D NOESY (Kumar et al., 1980), except that selective nitrogen pulses (applied as 90° rectangular pulses of duration 0.925 ms) centered at the arginine N^ϵ chemical shift (85 ppm) were used to ensure that only NOEs involving an arginine H^ϵ proton were detected. Assignment of the nearly degenerate Arg 18, 37, 39, and 59 N^ϵ−H^ϵ cross-peaks in imidazole buffer and N^η−H^η cross-peaks in imidazole and phosphate buffers (except Arg 37 N^η−H^η peaks in phosphate) was not pursued. ^{1}H−^{15}N HSQC spectra of the free SH2 domain dissolved in imidazole and phosphate buffer are shown in Figure 1a,b respectively, while the HSQC spectrum of the PLCC−pY1021 complex in imidazole buffer is illustrated in Figure 1c. Assignments are also provided in Figure 1.

Relaxation. Arginine N^ϵ T_1 and T_2 relaxation times, steady state $^{15}N^\epsilon\{^1H^\epsilon\}$ NOEs, and C^ζ $T_{1\varrho}$ relaxation times were determined by using ^{15}N−^{1}H correlation spectra with previously described modifications (Farrow et al., 1994; Yamazaki et al., 1994). ^{15}N T_1 values were obtained from a series of spectra acquired with delays of 11, 67, 153, 255, 366, 488, 655, and 855 ms. N^ϵ T_2 experiments included a CPMG (Carr & Purcell, 1954; Meiboom & Gill, 1958) period immediatley prior to ^{15}N chemical shift measurement. Spectra were recorded with CPMG periods of 16, 33, 50, 66, 83, 99, 116, and 132 ms. C^ζ $T_{1\varrho}$ experiments were performed by transferring magnetization from the $^1H^\epsilon$ proton to the $^{13}C^\zeta$ carbon via a set of INEPT (Morris & Freeman, 1979) transfers. Following a ^{13}C spin-lock period, during which the decay of carbon magnetization is measured, the magnetization is subsequently transferred back to the H^ϵ proton for detection. The transfer pathway is summarized as follows:

$$H^\epsilon \xrightarrow{J_{HN}} N^\epsilon(t_1) \xrightarrow{J_{N^\epsilon C^\zeta}} {}^{13}C^\zeta \xrightarrow{J_{N^\epsilon C^\zeta}} N^\epsilon \xrightarrow{J_{HN}} H^\epsilon(t_2) \quad (1)$$

with the appropriate scalar coupling constants involved in the magnetization transfer process indicated about the arrows; t_1 and t_2 are the acquisition times. Note that, during the spin-lock period, the magnetization of interest is of the form $2C_x^\zeta N_z^\epsilon$, where C_x^ζ and N_z^ϵ are the transverse and longitudinal components of $^{13}C^\zeta$ and $^{15}N^\epsilon$ magnetization, respectively. Therefore, the measured relaxation rate $T_{1\varrho}^{meas}$ is given by

$$1/T_{1\varrho}^{meas} = 1/T_{1\varrho}C^\zeta + 1/T_1^N \quad (2)$$

where $1/T_{1\varrho}C^\zeta$ is the sought-after relaxation rate and T_1^N is the longitudinal relaxation time of the directly bound N^ϵ nitrogen. Spectra were recorded with spin-lock periods of 10, 20, 60, 100, 150, and 200 ms.

N^ϵ−H^ϵ cross-peak intensities from the preceding three sets of experiments were measured, and the resulting decay curves were fit to simple exponential functions to obtain values for N^ϵ T_1, N^ϵ T_2, and C^ζ $T_{1\varrho}$ relaxation times (Farrow et al., 1994). Steady state $^{15}N^\epsilon\{^1H^\epsilon\}$ NOE values were determined from spectra where magnetization originates on the ^{15}N spins according to the relation NOE = I(SAT)/I(NOSAT), where I(SAT) is the intensity of a cross-peak in the spectrum recorded with 3 s of ^{1}H saturation and I(NOSAT) is the intensity of the corresponding peak in the absence of saturation. A recycle delay of 5 s was employed for both SAT and NOSAT spectra. All of the spectra for measurement of relaxation properties were acquired at 500 MHz with acquisition times of 32.0 ms and 128 complex points in T_1 (^{15}N) and 64.0 ms and 512 complex points in t_2 (^{1}H), except for C^ζ $T_{1\varrho}$ measurements, which were recorded with acquisition times of 20.0 ms and 80 complex points in t_1 (^{15}N). All of the T_1 and T_2 spectra were recorded in such a manner that the nonoptimal delay between scans will affect only the sensitivity and not the measurement of the relevant relaxation parameter (Sklenar et al., 1987). An additional set of N^ϵ T_2 experiments was performed at 600 MHz in order to assess the contribution of slow motions to measured T_2 values. These experiments utilized the same length of CPMG periods described earlier and acquisition times of 26.7 ms and 128 complex points in t_1 (^{15}N) and 64.0 ms and 576 complex points in t_2 (^{1}H).

Table 1: Arginine Order Parameters, H^{ϵ} Exchange Rates, and Accessible Surface Area for PLCC SH2−pY1021 Complex

residue	N^{ϵ} order parameter (S^2)	k_N (s^{-1})[a]	k_R (s^{-1})[b]	accessible surface area per residue ($Å^2$)[c]
R18	0.72 ± 0.01	0.01−0.7[d]		86 ± 30
R27	0.26 ± 0.04	18.6 ± 1.9	23.0 ± 1.4	169 ± 14
R30	*e*	30.0 ± 2.8	41.2 ± 2.7	153 ± 30
R37	0.80 ± 0.01	0.00086 ± 0.00001[f]		0.6 ± 1.4
R39	0.68 ± 0.03	0.01−1.3[g]		58 ± 17
R50	0.59 ± 0.04	2.6 ± 0.7	1.7 ± 1.0	44 ± 10
R59	0.31 ± 0.01	7.3 ± 0.7	9.8 ± 2.0	70 ± 21
R91	0.37 ± 0.02	14.1 ± 1.1	15.9 ± 4.4	130 ± 27
R96	0.27 ± 0.03	46.5 ± 8.9	52.7 ± 3.2	156 ± 26

[a] H^{ϵ} exchange rate as measured by NOE experiments (Grzesiek & Bax, 1993). [b] H^{ϵ} exchange rate as measured by ROE experiments (Grzesiek & Bax, 1993). [c] Average accessible surface area calculated from an ensemble of 24 structures generated via standard NOE-based procedures (Pascal et al., manuscript in preparation). [d] Exchange rate too slow (<0.7 s^{-1}) for measurement of k_N and k_R and too rapid (>0.01 s^{-1}) for measurements via D_2O exchange. [e] Data for R30 could not be fit by any of the models. [f] Exchange rate measured from the rate of disappearance of the NH cross-peak in D_2O sample. [g] Exchange rate too slow (<1.3 s^{-1}) for measurement of k_N and k_R and too rapid (>0.01 s^{-1}) for measurement via D_2O exchange.

Five alternate models for the spectral density function, $J(\omega)$, were used to fit the experimental values of N^{ϵ} T_1, T_2, and steady state $^{15}N^{\epsilon}\{^1H^{\epsilon}\}$ NOEs (Farrow et al., 1994). All of the models are based on the spectral density function of Lipari and Szabo (1982a,b), which in its simplest form includes a generalized order parameter, S, and an effective correlation time, τ_e. The first model includes only the generalized order parameter (S) with $\tau_e = 0$, while the second model includes both S and τ_e. The effects of millisecond-microsecond time scale motions (R_{ex}) are included in the third and fourth models. In model 3, S and R_{ex} are fit, while S, R_{ex}, and τ_e are fit in model 4. The fifth model includes two high-frequency motions separated by at least 1 order of magnitude (Clore et al., 1990a,b). The square of the order parameter from the model with the smallest number of variable parameters that fit the T_1, T_2, and NOE values to within experimental error is presented in Table 1.

Exchange. Arginine H^{ϵ} exchange rates with solvent water for the PLCC SH2−pY1021 complex were determined by a combination of two complementary techniques. Very rapid (k_{ex} > ~1.0 s^{-1}, where k_{ex} is the NH exchange rate) H^{ϵ} exchange rates were measured by analysis of a series of ^{15}N−^1H correlation spectra acquired in the presence and absence of a selective water proton inversion period followed by a NOESY (τ_{mix} = 20, 40, 60, 75, and 85 ms) or ROESY (τ_{mix} = 15, 30, 45, and 55 ms) mixing period (Grzesiek & Bax, 1993). N^{ϵ}−H^{ϵ} cross-peaks from residues in which the H^{ϵ} rapidly exchanges with water show large differences in spectra acquired with and without water inversion. Comparison of NOESY and ROESY spectra distinguishes H^{ϵ}−water proton exchange from dipolar magnetization exchange (NOE or ROE to water). N^{ϵ}−H^{ϵ} cross-peak intensities were measured, and the resulting decay curves were fit to simple exponential functions to obtain exchange rates. Spectra were recorded with acquisition times of 24.0 ms and 96 complex points in t_1 (^{15}N) and 64.0 ms and 512 complex points in t_2 (^1H).

In order to measure the H^{ϵ} exchange rates of very slowly exchanging protons ($\tau_{ex} \geq$ minutes, where τ_{ex} is the exchange lifetime), a sample of 1.2 mM ^{15}N-labeled PLCC SH2 with equimolar unlabeled pY1021 in 100 mM sodium phosphate was prepared by lyophilizing from 90% H_2O/10% D_2O and redissolving in 100% D_2O. The rate of disappearance of ^1H resonances due to deuterium exchange was monitored by using short (5 min), enhanced sensitivity ^{15}N−^1H correlation spectra acquired at 600 MHz, with acquisition times of 26.3 ms and 64 complex points in t_1 (^{15}N carrier at 110 ppm) and 67.6 ms and 608 complex points in t_2 (^1H).

RESULTS

Relaxation. The PLCC SH2 domain contains nine arginine residues, four of which are located in the pTyr-binding pocket (arginines 18, 37, 39, and 59). The other arginines reside in loop or turn regions distant from the pTyr-binding site. The motion of the guanidino group can be probed, in part, by observation of the dynamic behavior of the N^{ϵ} and C^{ζ} atoms. ^{15}N relaxation studies of the arginine N^{ϵ} nitrogen are straightforward to interpret since the relaxation is primarily due to the $^{15}N^{\epsilon}$−$^1H^{\epsilon}$ dipolar interaction with a small contribution from chemical shift anisotropy (Allerhand et al., 1971). Cross-correlation effects between ^1H−^{15}N dipolar interactions involving the two η protons, however, can complicate the interpretation of N^{η} relaxation parameters in terms of dynamics. In contrast to protonated heteroatoms, the relaxation rates of $^{13}C^{\zeta}$ carbons are dominated by contributions from chemical shift anisotropy and dipole−dipole interactions involving proximal spins. For this reason, it is more difficult to interpret the dynamic behavior of such nuclei, and the $^{13}C^{\zeta}$ $T_{1\rho}$ values that have been obtained are used to provide only a qualitative measure of the motion.

The results of the $^{15}N^{\epsilon}$ relaxation study of the PLCC SH2−pY1021 complex are illustrated in Figure 2, where $^{15}N^{\epsilon}$ T_1 and T_2 relaxation times as well as steady state $^{15}N^{\epsilon}\{^1H^{\epsilon}\}$ NOE values are plotted for the nine arginine residues in PLCC SH2. Measurements were made at 500 MHz (^1H frequency) with the exception of ^{15}N T_2 values which were recorded at both 500 and 600 MHz. Rapid exchange between conformations results in a contribution to the transverse relaxation rate that scales as the square of ω_{ex}, the N^{ϵ} chemical shift difference between conformers measured in radians second^{-1} (Luz & Meiboom, 1963; Bloom et al., 1965). Since ω_{ex} is proportional to field strength, the equivalence of the measured $^{15}N^{\epsilon}$ T_2 values at 500 and 600 MHz to within experimental error (Figure 2b) suggests that exchange contributions will not complicate interpretation of the measured relaxation parameters. The relatively long T_1 and T_2 values and negative $^{15}N^{\epsilon}\{^1H^{\epsilon}\}$ NOEs observed for arginines 27, 30, 59, 91, and 96 indicate that these side chains undergo internal motions on the nanosecond to picosecond time scale, in addition to global reorientation. An overall correlation time of 6.6 ± 0.2 ns was determined by fitting data from 24 well-resolved backbone resonances from the same ^{15}N relaxation spectra. The relatively small T_1 and T_2 values and positive $^{15}N^{\epsilon}\{^1H^{\epsilon}\}$ NOE values observed for arginines 18, 37, 39, and 50 indicate that these residues are more constrained than the other arginines in the complex.

A more quantitative estimate of the amplitude of the motions can be obtained by extracting order parameters (Lipari & Szabo, 1982a,b), as described in the Materials and Methods section. Table 1 lists the values of S^2 obtained for each of the arginine residues in the PLCC SH2−pY1021

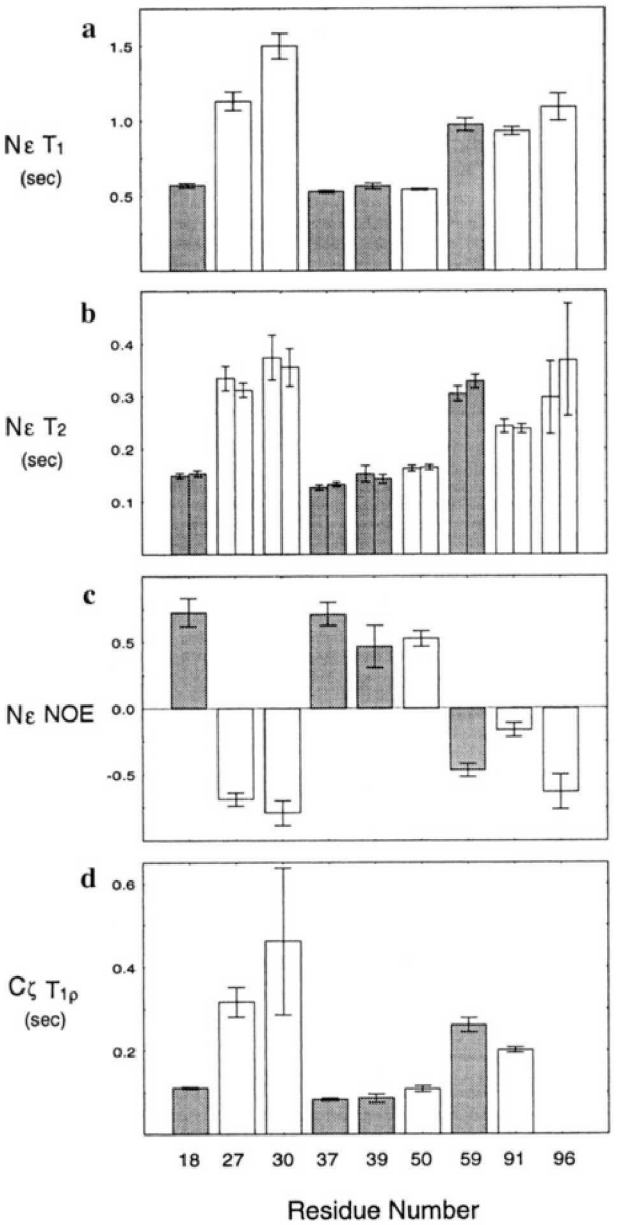

FIGURE 2: N^{ϵ} T_1 and T_2, steady state $^{15}N^{\epsilon}\{^1H^{\epsilon}\}$ NOE, and $T_{1\varrho}$ of C^{ζ} nuclei of PLCC SH2−pY1021 arginines. Data for residues within the pTyr-binding pocket are shaded. T_2 values were determined at 500 (left) and 600 MHz (right) field strengths. All other parameters are based on data measured at 500 MHz field strength. (The $T_{1\varrho}$ of Arg 96 C^{ζ} could not be determined accurately due to low signal-to-noise ratios.)

complex, along with the accessible surface area of each residue (Lee & Richards, 1971) calculated with the program X-PLOR (Brünger, 1992). S^2 values for the Arg 18, 37, 39, and 50 $^1H^{\epsilon}-^{15}N^{\epsilon}$ bond vectors range from 0.59 to 0.80, indicating that the amplitudes of the fast time scale motions (picosecond to nanosecond) of these vectors are only slightly larger, on average, than those of the backbone amide $^1H-^{15}N$ vectors (Farrow et al., 1994). The much smaller order parameters of Arg 27, 59, 91, and 96 $^1H^{\epsilon}-^{15}N^{\epsilon}$ vectors (S^2 = 0.26−0.37) indicate that these residues are much more mobile on a nanosecond to picosecond time scale. The data from Arg 30 could not be fit by any of the models, but it is clear from Figure 2 that it is highly disordered. Values of model-free parameters used to fit the data in Figure 2, including the explicit model used and the values of the correlation times extracted, are available as supplementary material.

The values of $T_{1\varrho}$ for $^{13}C^{\zeta}$, obtained from eq 2, are plotted in Figure 2d. Note that a $T_{1\varrho}$ value was not obtained for Arg 96 $^{13}C^{\zeta}$ due to the low sensitivity of the Arg 96 cross-peaks in the $T_{1\varrho}$ spectra. The smaller $^{13}C^{\zeta}$ $T_{1\varrho}$ values for arginines 18, 37, 39, and 50 indicate that the motions of the C^{ζ} carbons of these residues are more constrained than is the case for arginines 27, 30, 59, and 91. These results are in full agreement with the conclusion of higher mobility of the guanidino groups of arginines 27, 30, 59, and 91 based on ^{15}N relaxation data.

H^{ϵ} Proton Exchange. The relaxation experiments described earlier probe motions with correlation times on the order of nanoseconds or faster. It is also possible to investigate slower processes via hydrogen exchange experiments. Fast H^{ϵ} proton−solvent exchange rates (~1−50 s^{-1}) were measured by using experiments that rely on the selective excitation of the water resonance according to the procedure of Grzesiek and Bax (1993). Exchange rates for H^{ϵ} protons with exchange lifetimes on the order of several minutes or larger were established by quantitating the rate of decay of NH magnetization after dissolving a fully protonated sample in D_2O. Protection from hydrogen exchange is consistent with burial of the H^{ϵ} proton and/or hydrogen bonding. The H^{ϵ} protons of arginines 27, 30, 91, and 96 exchange at a rate >15 s^{-1}, and the exchange rate for Arg 59 is approximately 10 s^{-1}, which is consistent with significant solvent exposure (Table 1). In contrast, the H^{ϵ} protons of arginines 18, 37, 39, and 50 exchange at rates of 2 s^{-1} or less. It is of interest to note the correlation between increased surface accessibility (SA) and exchange rates, as well as the trend of decreased S^2 values with increased SA. To the extent that H^{ϵ} exchange rates provide a measure of slow motions, the correlation between S^2 and exchange rates (i.e., fast and slow motions, respectively) is noteworthy. It is likely that restriction of fast as well as slow motions is due to packing constraints, as indicated by the SA values in Table 1, possibly correlated with the formation of hydrogen bonds.

Chemical Shift. Chemical shift dispersion in proteins is the result of variable magnetic susceptibilities of the different chemical constituents in the molecule. Two of the most important effects are due to local fields caused by hydrogen bonds and to ring current effects of aromatic residues [Johnson & Bovey, 1958; for a review, see Haigh and Mallion (1980)]. Considerable effort is currently directed toward developing efficient algorithms for exploiting the rich amount of structural information available from chemical shifts (e.g., Wishart & Sykes, 1994). Here we have used the changes in chemical shifts between the free PLCC SH2 domain in 100 mM imidazole buffer (Figure 1a), the free domain in 100 mM phosphate buffer (Figure 1b), and the complex with pY1021 in imidazole buffer (Figure 1c) in order to characterize the structure of the phosphotyrosine-binding interface region.

The spectrum of the free PLCC SH2 domain in 100 mM imidazole buffer shows that the four $N^{\epsilon}-H^{\epsilon}$ cross-peaks from the guanidino groups of arginines in the pTyr-binding pocket, within the region defined by the oval in Figure 1a, are nearly degenerate. There is also significant overlap of $N^{\eta}-H^{\eta}$ cross-peaks.

It has been shown that in the absence of peptide, the phosphotyrosine-binding site of the Src SH2 domain contains

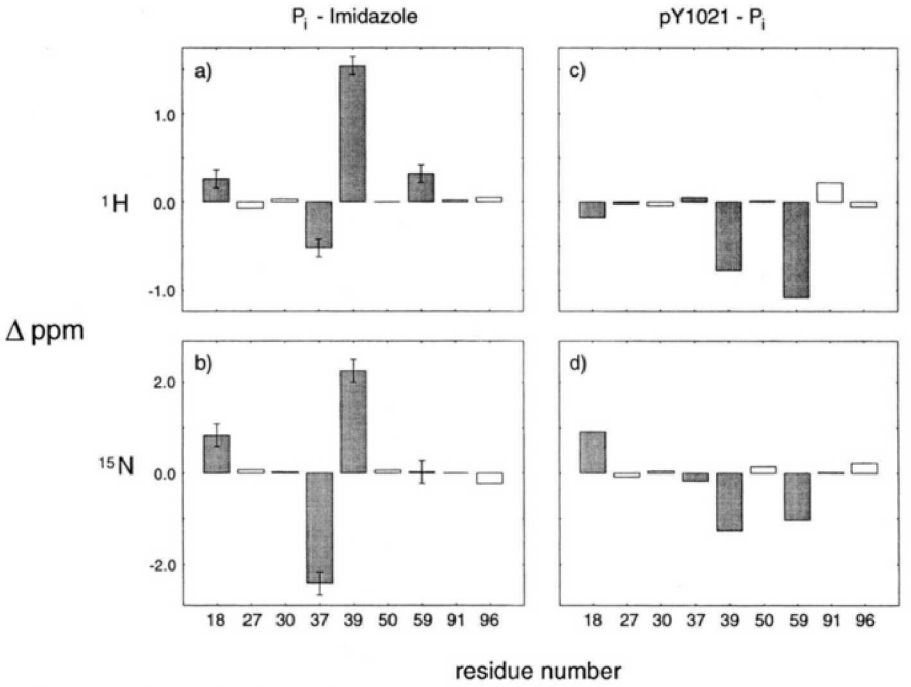

FIGURE 3: Chemical shift changes in arginine H^ϵ and N^ϵ resonances from Figure 1. The graphs labeled P_i − imidazole represent the differences between Figure 1b and 1a, isolating the effect of the phosphate. The graphs labeled pY1021 − P_i represent differences in chemical shifts between Figure 1c and 1b, indicating the effect of the remainder of the peptide, predominantly the pTyr aromatic ring. Error bars are used to account for the unassigned peaks in Figure 1a (Arg 18, 37, 39, and 59).

a phosphate in two of the four independent molecules of the crystalline unit cell, with interactions that mimic the SH2−phosphotyrosine contacts (Waksman et al., 1993). In solution, the presence of a stably bound phosphate ion can lead to large chemical shift changes in nearby spins, particularly when a hydrogen bond to phosphate is formed. It is apparent from the chemical shift changes in the N^ϵ−H^ϵ cross-peaks of arginines 18, 37, 39, and 59 in 100 mM phosphate buffer (Figure 1b) relative to imidazole buffer (Figure 1a) and the absence of large changes in any of the other H^ϵ and N^ϵ chemical shifts that buffer phosphate interacts primarily with the arginines in the pTyr pocket. Most striking is the appearance of cross-peaks corresponding to one of the two NH_2 groups of Arg 37. Cross-peaks from the other Arg 37 NH_2 group are not observed in spectra recorded at 30 °C, but they are present at 10 °C and demonstrate chemical shifts similar to those observed in the PLCC SH2−pY1021 complex. The chemical shift changes of the arginine guanidino H^ϵ and N^ϵ resonances that occur upon substitution of phosphate for imadizole buffer are shown in Figure 3a,b. The largest chemical shift changes involve Arg 37 and Arg 39. The downfield shifts of the two N^η resonances of Arg 37 and one of the two H^η protons of each N^η are consistent with the formation of two hydrogen bonds to the phosphate ion; the slowed rotations about the C^ζ−N^η bonds break the degeneracy or near degeneracy of the H^η chemical shifts observed in imidazole buffer. The temperature dependence of the second set of N^η−H^η resonances may be due to intermediate exchange broadening caused by more rapid rotation about the second C^ζ−N^η bond. The H^ϵ and N^ϵ resonances of Arg 39 shift 1.5 and 2.2 ppm downfield, respectively, and are consistent with the formation of a hydrogen bond between an oxygen of the phosphate ion and the H^ϵ. The Arg 37 H^ϵ and N^ϵ resonances shift upfield possibly due to the breaking of a intramolecular hydrogen bond that exists in the absence of phosphate or phosphopeptide or due to some other interaction mediated by the presence of the Arg 37 N^η−phosphate hydrogen bonds. The H^ϵ and N^ϵ resonances of Arg 18 and the H^ϵ resonance of Arg 59 shift downfield; these shifts may reflect weak or exchanging hydrogen bonds to the phosphate ion. The Arg 96 H^ϵ and N^ϵ chemical shifts also change slightly upon substitution of phosphate for imidazole buffer. This may be due to an interaction between phosphate and the Arg 96 guanidino group, possibly stabilized by the presence of the Lys 94 side chain in close vicinity.

Several changes in arginine guanidino chemical shifts occur when a 1:1 molar ratio of pY1021 phosphopeptide is added to the PLCC SH2 domain sample in 100 mM imidazole buffer (Figure 1c). The large differences in affinities of PLCC SH2 for the pY1021 peptide (~100 nM) and phosphate (millimolar; Piccione et al., 1993; S. E. Shoelson, personal communication) dictate that, in the presence of peptide, the binding site is saturated with pY1021 and not phosphate, even in excess phosphate buffer. Imidazole buffer was used in place of phosphate buffer for these chemical shift studies, however, to ensure that this is the case. Additional confirmation is provided by the fact that the chemical shifts of residues in the binding site are essentially unaffected upon a change of buffer in the presence of peptide.

The differences between the chemical shifts in spectra shown in Figure 1b,c can be attributed to the non-phosphate portion of the peptide, assuming that the phosphate portion of pY1021 binds to the SH2 domain in the same manner as free phosphate (see above). These differences are shown in Figure 3c,d for H^ϵ and N^ϵ chemical shifts, respectively. The NOE-based structure of the complex (Pascal et al., 1994) establishes that interactions between the peptide and the side chains of arginines 37, 39, and 59 can only involve the pTyr residue of the peptide, while Arg 18 may contact pTyr or residues N-terminal to the pTyr. Resonances of groups

interacting with the pTyr ring can be shifted significantly due to the effects of the aromatic π-electron cloud. The upfield shifts of the N^{ϵ} and H^{ϵ} resonances of Arg 39 and Arg 59 (Figure 3c,d) suggest that the position of these groups is axial to (above or below) the plane of the ring. An Arg 18 $N^{\eta}-H^{\eta}$ cross-peak has also shifted upfield, suggesting that this group may interact with the ring in an axial manner as well. It is difficult to speculate on the positioning of the Arg 18 $N^{\epsilon}-H^{\epsilon}$ group on the basis of chemical shift changes.

Upon the addition of peptide, two Arg 39 $N^{\eta}-H^{\eta}$ cross-peaks can be seen at slightly different ^{15}N and very different ^{1}H chemical shifts. This indicates that rotation about the Arg 39 $N^{\epsilon}-C^{\zeta}$ bond has been slowed considerably in the complex. The movement of one of the two $N^{\eta}-H^{\eta}$ cross-peaks of Arg 39 to downfield proton chemical shift values suggests that this H^{η} proton may lie in the plane of the pTyr ring. Although the chemical shifts of the Arg 37 guanidino proton and nitrogen cross-peaks are virtually unchanged between free SH2 in phosphate and the SH2–pY1021 complex, the second pair of $N^{\eta}-H^{\eta}$ cross-peaks now rises above the noise at 30 °C while the first pair of peaks also becomes sharper, suggesting that rotation about both $C^{\zeta}-N^{\eta}$ bonds has been slowed. Note, however, that the second pair of peaks is still less intense than the first pair. The evidence suggests that Arg 37 in the SH2–pY1021 complex interacts with the peptide primarily via two phosphate–H^{η} hydrogen bonds (one from each NH_2 group) of slightly different stabilities. This is similar to the Arg 37 interaction with free phosphate, except that both hydrogen bonds are somewhat stabilized by the presence of the remainder of the peptide.

Aliphatic Broadening. Figure 4 illustrates $^{15}N-^{1}H$ strips taken from the 3D H(CCO)NH TOCSY experiment showing cross-peaks from a number of the arginines in the PLCC SH2 domain. The peaks along F_1 represent aliphatic resonances from the residue specified along the x-axis. Examination of the spectrum shows that there is significant line broadening of the aliphatic resonances of arginines 18 (not shown due to spectral overlap), 37, 39, 50, and 59. The broadening implies that intermediate (millisecond–microsecond) time scale chemical exchange between different environments is present in the pTyr-binding pocket as well as near Arg 50, which is not located within the binding site. Resonances of arginines 27, 30, 91 (not shown due to spectral overlap), and 96 and other non-arginine side chains (data not shown) are much more intense with no apparent evidence of exchange broadening.

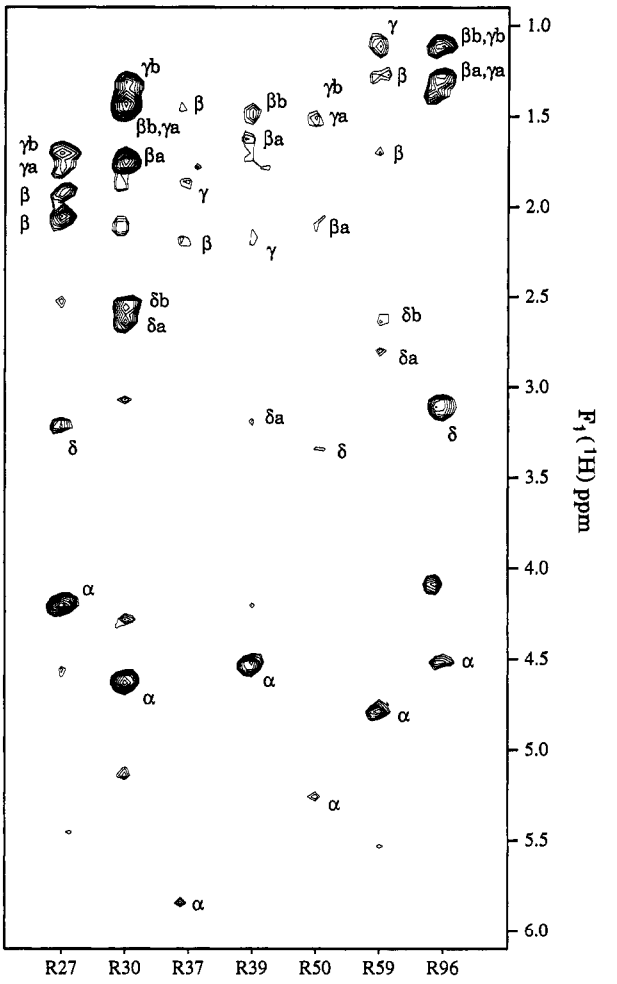

FIGURE 4: Amide strips of arginine residues of the PLCC SH2–pY1021 complex taken from the H(CCO)NH TOCSY spectrum (0.8 mM PLCC SH2–pY1021 in 100 mM sodium phosphate, pH 5.7). Many peaks for arginines 18, 37, 39, 50, and 59 are of low intensity, which is indicative of intermediate chemical exchange broadening. (Peaks for Arg 18 and Arg 91 are not shown due to spectral overlap.)

DISCUSSION

The dynamics of arginine $N^{\epsilon}-H^{\epsilon}$ groups, as monitored by $^{15}N^{\epsilon}$ relaxation properties and H^{ϵ} hydrogen exchange rates coupled with the chemical shift changes that occur upon the binding of phosphate or pY1021 peptide to PLCC SH2, allow a much more detailed description of the pTyr-binding site than is possible using an approach exclusively based on NOE studies. The available data strongly suggest that the arginines can be divided into a number of distinct groups. The first group of residues includes arginines 27, 30, 91, and 96. The $N^{\epsilon}-H^{\epsilon}$ bond vectors of these arginines have significant high-frequency (nanosecond–picosecond) motions, characterized by low values of S^2, and show no evidence of intermediate time scale motion in spectra that record aliphatic proton shifts. These residues do not interact with pTyr and are highly solvent exposed, as judged by hydrogen exchange rates and calculated accessible surface areas. A second group of arginines consists of residues 18, 37, and 39. These residues are relatively solvent inaccessible, interact with pTyr, and have slowed rotations about the $N^{\epsilon}-C^{\zeta}$ bond within the guanidino group, as established by the observation of two distinct N^{η} chemical shifts for each residue (Yamazaki et al., 1995). Only one Arg 18 $N^{\eta}-H^{\eta}$ peak is labeled in Figure 1c because the H^{η} resonances of the second group are broadened to below the noise. In the case of Arg 37, hydrogen bonding with the phosphate of the pY1021 peptide slows rotation about the $C^{\zeta}-N^{\eta}$ bonds as well, to the point where distinct proton chemical shifts are observed for each of the four H^{η} protons. The order parameters for the $N^{\epsilon}-H^{\epsilon}$ bonds of these residues are considerably larger than those for the first class of arginines, and there is significant broadening of aliphatic chemical shifts in the H(CCO)NH TOCSY experiment due to intermediate time scale dynamics. The dynamic behavior and the hydrogen exchange data for Arg 50 are similar to those of residues in the second group of arginines, although it clearly does not interact with the pTyr. In contrast, ^{15}N relaxation studies indicate considerable high-frequency motion at the N^{ϵ} position of Arg 59, while

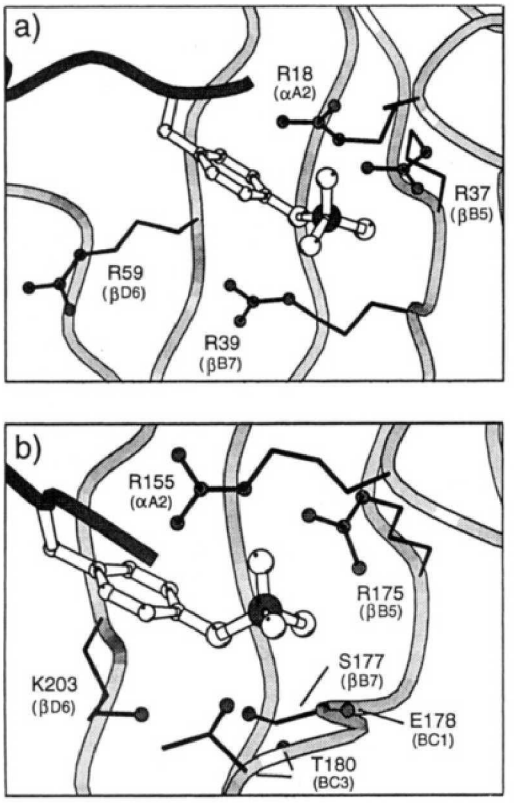

FIGURE 5: Schematic diagrams of (a) the PLCC SH2 pTyr-binding pocket and (b) the Src SH2 pTyr-binding pocket (Waksman et al., 1993) generated with MOLSCRIPT (Kraulis, 1991). Backbone traces of the SH2 domains are drawn as light gray strings. The peptide backbone is drawn as a darker string, with the pTyr side chain in ball-and-stick mode. SH2 side chains that interact with pTyr are pictured in stick form (side chain O and N and arginine C^{ζ} atoms are drawn as dark balls). The PLCC SH2 structure is one member of an ensemble of structures generated via standard NOE-based procedures (Pascal et al., 1994) that is consistent with the results of relaxation, exchange, and chemical shift data. In (b), backbone nitrogens of Glu 178 and Thr 180 form hydrogen bonds to phosphate and are drawn as dark balls. The nomenclature from Eck et al. (1993) is furnished (in parentheses) for comparison. For clarity, all hydrogen atoms have been omitted.

the aliphatic ^{1}H and ^{13}C chemical shifts are significantly broadened by intermediate time scale motion.

Both NH_2 groups of Arg 37 serve as proton donors in the formation of stable hydrogen bonds with the phosphate of the pY1021 peptide. However, intensity differences between the $N^{\eta}-H^{\eta}$ cross-peaks (see Figure 1b,c) due to differential broadening imply differences in the restriction of motion about the two $C^{\zeta}-N^{\eta}$ bonds. This suggests that one of the hydrogen bonds is considerably more stable than the other. The chemical shift data are also consistent with the formation of an Arg 39 H^{ϵ}−phosphate hydrogen bond. It is clear from the chemical shift changes that occur upon substitution of the pY1021 peptide for phosphate in the binding site that the guanidino groups of arginines 39, 59, and possibly 18 interact with the pTyr ring. These results are consistent with, but complementary to, the recently refined structure of the PLCC SH2−pY1021 complex derived from NOE and scalar coupling data (Pascal et al., manuscript in preparation). Figure 5a illustrates the pTyr-binding site of the complex from one structure of the calculated ensemble, which is consistent with the present data.

The broadening of the aliphatic resonances of arginines 18, 37, 39, 50, and 59 (see Figure 4) suggests that these chemical shifts are modulated by motion occurring on a millisecond−microsecond time scale. While four arginine side chains line the pTyr-binding site in the PLCC SH2 domain (18, 37, 39, and 59), in the Src SH2 domain only positions analogous to Arg 18 and Arg 37 are conserved, with residues at the positions of Arg 39 and Arg 59 replaced by Ser and Lys, respectively. In the SH2 domain from the Syp phosphatase, only the position corresponding to Arg 37 is conserved (Marenger & Pawson, 1992). The multiplicity of possible arginine−phosphate interactions in the PLCC SH2 complex could result in hydrogen bond exchange, leading to the observed broadening of aliphatic resonances. However, since the contribution to the $^{15}N^{\epsilon}$ transverse relaxation rate from exchange is proportional to the square of ω_{ex} (the N^{ϵ} chemical shift difference between conformers measured in radians second^{-1}) and ω_{ex} scales as the field strength, the equivalence of $^{15}N^{\epsilon}$ T_2 values measured at 500 and 600 MHz (see Figure 2b) seems to suggest that chemical shift-modulating behavior is absent at the guanidino groups. However, these results only require either that ω_{ex} for each Arg N^{ϵ} be very small or that the conformational exchange causing N^{ϵ} chemical shift modulation occurs on a time scale that does not result in different measured N^{ϵ} T_2 values at 500 and 600 MHz.

Bloom et al. (1965) derived equations to fit the dependence of the measured ^{15}N transverse relaxation rates on the spacing between 180° pulses in the CPMG sequence. By assuming a value of 50 Hz for $\omega_{ex}/2\pi$, which is consistent with changes in ^{15}N chemical shift caused by hydrogen bonding (Figures 1 and 3) and ω_{ex} values determined experimentally for a fragment of bacteriorhodopsin (Orekhov et al., 1994), these equations show that the exchange rate, k_{ex}, must be in the range of $\sim 200\ s^{-1} < k_{ex} < \sim 10^4\ s^{-1}$ for the exchange effects to cause significant differences in the arginine N^{ϵ} T_2 values reported here at 500 and 600 MHz. If $\omega_{ex}/2\pi$ is less than 50 Hz, the minimum value of k required to cause observable differences at 500 and 600 MHz would increase to more than 200 s^{-1}. Therefore, a model involving exchange between a hydrogen-bonded and a non-hydrogen-bonded configuration of a given $N^{\epsilon}-H^{\epsilon}$ group with $k_{ex} < 200\ s^{-1}$ and $\omega_{ex}/2\pi < \sim 50$ Hz is consistent with these results. A second model involves the $N^{\epsilon}-H^{\epsilon}$ group of a given residue participating in hydrogen bonds to various exchanging acceptor groups. This is likely to cause less chemical shift modulation (small ω_{ex}) due to the similarity of the N^{ϵ} environments, and thus k_{ex} may be greater than 200 s^{-1}. A third model presumes stable phosphotyrosine−guanidino hydrogen bonds, with the broadening of aliphatic resonances resulting from motion of this intact region. In this case, the aliphatic regions of the arginines may act as flexible linkers that adjust to the relocation of the pTyr−guanidino complex. Once again, due to the similarity of the N^{ϵ} environments, ω_{ex} may be small and k_{ex} may be greater than 200 s^{-1}. Each of the preceding models could result in broadening of the aliphatic resonances from Arg 59 that contact the aromatic portion of pTyr, although the Arg 59 guanidino group does not have a stable hydrogen bond to phosphate. Finally, the actual dynamics may be represented by some combination of these models and may also include exchanging hydrogen bonds from arginine $N^{\eta}-H^{\eta}$ groups.

The broadening of aliphatic arginine side chains is not limited to those residues that line the binding site. Arg 50 side chain resonances have reduced intensity in the H(CCO)-

NH TOCSY experiment (Figure 4). Inspection of the structure of the PLCC SH2−pY1021 complex indicates that the Arg 50 guanidino group is within hydrogen-bonding distance to carbonyl groups of Leu 25, Met 26, Val 28, Pro 29, Arg 30, and Gly 53. The carbonyl groups of these residues are not stably hydrogen bonded to backbone atoms. The formation of transient hydrogen bonds to two or more of the carbonyl groups and exchange between these hydrogen-bonding configurations could explain the broadening of the resonances of Arg 50, analogous to the proposed exchanging hydrogen-bonding configurations within the pTyr-binding pocket.

Comparison with the Structure of a Src SH2−Phosphopeptide Complex. Figure 5 illustrates the structures of the pTyr-binding pockets of PLCC SH2−pY1021 and the Src SH2 domain in complex with a peptide containing the sequence pYEEI (Waksman et al., 1993). The analogous residues in the pTyr-binding sites of the PLCC SH2 and Src SH2 domains, with nomenclature specifying positioning within secondary structural elements (Eck et al., 1993), are αA2 (Arg 18 and Arg 155), βB5 (Arg 37 and Arg 175), βB7 (Arg 39 and Ser 177), and βD6 (Arg 59 and Lys 203). Arg αA2 in the Src complex forms a number of hydrogen-bonding interactions; the first is between the phosphate and the H^{ϵ} guanidino proton, and the second is between an H^{η} proton and the carbonyl of the residue immediately N-terminal to the pTyr. In addition, the orientation of the guanidino group and the pTyr of the peptide allows a strong amino−aromatic interaction involving an H^{η} proton. The NMR-derived data for the PLCC SH2−pY1021 complex are consistent with these results for the Src structure. In both complexes, the NH_2 groups of arginine βB5 donate hydrogen bonds to the phosphate of the pTyr in the peptide. The Ser βB7 hydroxyl group in the Src structure hydrogen bonds to the phosphate, as does the H^{ϵ} proton of Arg βB7 in the PLCC complex. The additional length of the Arg βB7 side chain in the PLCC complex may prevent the backbone of the loop connecting β-strands B and C (the BC loop) from approaching the phosphate region as closely as in the Src complex, possibly contributing to weakening or elimination of the BC loop backbone amide−phosphate hydrogen bonds observed in Src. In this regard it is important to note that we have found no evidence of either chemical shift changes or changes in the dynamics of the BC loop in the PLCC SH2 domain upon peptide binding (Farrow et al., 1994). Both Arg βD6 in PLCC SH2 and Lys βD6 in Src SH2 interact with pTyr primarily through aliphatic−aromatic interactions. In the Src complex, a threonine hydroxyl from the BC loop hydrogen bonds to the side chain amino group of Lys βD6. We have found no evidence of the analogous interaction of the PLCC Arg βD6 guanidino group with the BC loop, consistent with the low Arg 59 N^{ϵ} order parameter, rapid H^{ϵ} exchange, and degeneracy of the Arg 59 $N^{\eta}-H^{\eta}$ cross-peaks.

In summary, measurements of arginine N^{ϵ} and C^{ζ} relaxation times, H^{ϵ} exchange, and guanidino group chemical shifts have enabled the characterization of the structure and dynamics of the pTyr-binding pocket of the PLCC SH2−pY1021 complex at a level that is not possible using only NOE connectivities and scalar coupling data. The results suggest that the arginines that line the binding site have distinct interactions with the pTyr of the peptide and display diverse motional properties over a wide range of time scales. The approach utilized here may be effective in the study of different SH2−peptide complexes and other arginine−phosphate interactions, such as those in DNA−protein and RNA−protein complexes.

ACKNOWLEDGMENT

We thank the laboratory of Steven S. Shoelsen for providing pY1021 peptide and Tony Pawson for his enthusiastic support. We also thank Neil Farrow for his help with the relaxation studies.

SUPPORTING INFORMATION AVAILABLE

Table containing full results of spectral density function parameters used to fit T_1, T_2, and NOE data (1 page). Ordering information is given on any current masthead page.

REFERENCES

Allerhand, A., Doddrell, D., & Komoroski, R. (1971) *J. Chem. Phys. 55,* 189.
Bax, A., & Pochapsky, S. (1992) *J. Magn. Reson. 99,* 638.
Bloom, M., Reeves, L. W., & Wells, E. J. (1965) *J. Chem. Phys. 42,* 1615.
Brünger, A. T. (1992) *X-PLOR Version 3.1: A System for X-Ray Crystallography and NMR,* Yale University Press, New Haven, CT.
Cantley, L. C., Auger, K. R., Carpenter, C., Duckworth, B., Graziani, A., Kapeller, R., & Soltoff, S. (1991) *Cell 64,* 281.
Carr, H. Y., & Purcell, E. M. (1954) *Phys. Rev. 4,* 630.
Clore, G. M., Driscoll, P. C., Wingfield, P. T., & Gronenborn, A. M. (1990a) *Biochemistry 29,* 7387.
Clore, G. M., Szabo, A., Bax, A., Kay, L. E., Driscoll, P. C., & Gronenborn, A. M. (1990b) *J. Am. Chem. Soc. 112,* 4989.
Delaglio, F. (1993) NMRPipe System of Software, National Institutes of Health, Bethesda, MD.
Eck, M. J., Shoelson, S. E., & Harrison, S. C. (1993) *Nature 362,* 87.
Farrow, N. A., Muhandiram, R., Singer, A. U., Pascal, S. M., Kay. C. M., Gish, G., Shoelson, S. E., Pawson, T., Forman-Kay, J. D., & Kay, L. E. (1994) *Biochemistry 33,* 5984.
Garrett, D. S., Powers, R., Gronenborn, A. M., & Clore, G. M. (1991) *J. Magn. Reson. 95,* 214.
Grzesiek, S., & Bax, A. (1993) *J. Biomol. NMR 3,* 627.
Grzesiek, S., Anglister, J., & Bax, A. (1993) *J. Magn. Reson. (B) 101,* 114.
Haigh, C. W., & Mallion, R. B. (1980) *Prog. NMR Spectrosc. 13,* 303.
Johnson, C. E., & Bovey, F. A. (1958) *J. Chem. Phys. 29,* 1012.
Kay, L. E. (1993) *J. Am. Chem. Soc. 115,* 2055.
Kay, L. E., Keifer, P., & Saarinen, T. (1992) *J. Am. Chem. Soc. 114,* 10663.
Koch, C. A., Anderson, D., Moran, M. F., Ellis, C., & Pawson, T. (1991) *Science 252,* 668.
Kraulis, P. (1991) *J. Appl. Cystallogr. 24,* 946.
Kumar, A., Ernst, R. R., & Wuthrich, K. (1980) *Biochem. Biophys. Res. Commun. 95,* 1.
Lee, B., & Richards, F. M. (1971) *J. Mol. Biol. 55,* 379.
Lipari, G., & Szabo, A. (1982a) *J. Am. Chem. Soc. 104,* 4546.
Lipari, G., & Szabo, A. (1982b) *J. Am. Chem. Soc. 104,* 4559.
Logan, T. M., Olejniczak, E. T., Xu, R. X., & Fesik, S. W. (1993) *J. Biomol. NMR 3,* 225.
Luz, Z., & Meiboom, S. (1963) *J. Chem. Phys. 39,* 366.
Marenger, L. E., & Pawson, T. (1992) *J. Biol. Chem. 267,* 22779.
Marion, D., Ikura, M., Tschudin, R., & Bax, A. (1989a) *J. Magn. Reson. 85,* 393.
Marion, D., Ikura, M., & Bax, A. (1989b) *J. Magn. Reson. 84,* 425.
Meiboom, S., & Gill, D. (1958) *Rev. Sci. Instrum. 29,* 688.
Montelione, G. T., Lyons, B. A., Emerson, S. D., & Tashiro, M. (1992) *J. Am. Chem. Soc. 114,* 10974.

Morris, G. A., & Freeman, R. (1979) *J. Am. Chem. Soc. 101,* 760.
Muhandiram, R., & Kay, L. E. (1994) *J. Magn. Reson. (B) 103,* 203.
Omichinski, J. G., Clore, G. M., Schaad, O., Felsenfeld, G., Trainor, C., Appella, E., Stahl, S. J., & Gronenborn, A. M. (1993) *Science 261,* 438.
Orekhov, V. Y., Pervushin, K. V., & Arseniev, A. S. (1994) *Eur. J. Biochem. 219,* 887.
Pascal, S. M., Singer, A. U., Gish, G., Yamazaki, T., Shoelson, S. E., Pawson, T., Kay, L. E., & Forman-Kay, J. D. (1994) *Cell 77,* 461.
Pavletich, N. P., & Pabo, C. O. (1993) *Science 261,* 1701.
Pawson, T., & Gish, G. D. (1992) *Cell 71,* 359.
Piccione, E., Case, R. D., Domchek, S. M., Hu, P., Chaudhuri, M., Backer, J. M., Schlessinger, J., & Shoelsen, S. E. (1993) *Biochemistry 32,* 3197.
Rhee, S. G. (1991) *Trends Biochem. Sci. 16,* 297.
Schleucher, J., Schwedinger, M., & Greisenger, C. (1993) *Angew. Chem. 105,* 1518.
Shaka, A. J., Lee, C. J., & Pines, A. (1988) *J. Magn. Reson. 64,* 547.
Sklenar, V., Torchia, D., & Bax, A. (1987) *J. Magn. Reson. 73,* 375.
Waksman, G., Shoelson, S. E., Pant, N., Cowburn, D., & Kuriyan, J. (1993) *Cell 72,* 779.
Wishart, D. S., & Sykes, B. D. (1994) *J. Biomol. NMR 4,* 171.
Yamazaki, T., Muhandiram, R., & Kay, L. E. (1994) *J. Am. Chem. Soc. 116,* 8266.
Yamazaki, T., Pascal, S. M., Singer, A. U., Forman-Kay, J. D., & Kay, L. E. (1995) *J. Am. Chem. Soc. 117,* 3556.
Zhu, G., & Bax, A. (1990) *J. Magn. Reson. 90,* 405.

BI951019V